

CHEMICAL CONTRAST IN SCANNING NEAR-FIELD OPTICAL MICROSCOPY

GERD KAUPP* AND ANDREAS HERRMANN

Organische Chemie I, FB 9, Universität Oldenburg, Postfach 2503, D-26111 Oldenburg, Germany

Repeatable and stable scanning near-field optical microscopy (SNOM) images are obtained under shear-force control if uncoated, i.e. cold and sharp, tapered fiber tips are used. True chemical contrast is seen for the first time on organic crystals due to the different near-field reflectivities of different chemical species on partly oxidized anthracene. The topography spans a Z-range of 500 nm. The surface roughness is tolerable and the sites of reaction can be related to crystal structure data. A submicroscopic local resolution of 18 nm has been obtained for chemical contrast, discriminating different chemical species even with poorly reflecting organics on rough crystal surfaces. Thus, reflection-back-to-the-fiber SNOM will find wide applications for both transparent and opaque samples. All drawbacks with blunt and hot metal-coated tips at a <10 nm distance from the surface in previous SNOM setups are overcome. © 1997 John Wiley & Sons, Ltd.

J. Phys. Org. Chem. **10**, 675–679 (1997) No. of Figures: 6 No. of Tables: 0 No. of References: 23

Keywords: chemical contrast; scanning near-field optical microscopy

Received 18 December 1996; revised 27 February 1997; accepted 27 February 1997

INTRODUCTION

Scanning near-field optical microscopy (SNOM or NSOM) beyond the diffraction limit¹ is considerably older than atomic force microscopy (AFM)² but it has not yet found the broad application of the latter. The strength of SNOM is its ability to provide local spectroscopic information in addition to the topographic information which is gained from simultaneous AFM control. Thus, looking for topography with SNOM by using constant height techniques is less profitable than local spectroscopy by running constant distance modes. If topographic features are excluded, the contrast depends only on the chemical composition or the physical state and local variations in reflected intensities provide further insight into the nature of submicroscopic surface features. This paper reports on the first interpretable chemical contrasts of SNOM on organic crystals, which discriminate different local surface compositions, observations that should assign to SNOM the importance that AFM and other SXM techniques already enjoy.

REFLECTION-BACK-TO-THE-FIBER SNOM

The detection of chemical contrast in the near-field requires stable conditions while the scanning tip is kept at a ≤ 10 nm

distance from an usually rough surface. Not all of the currently available tip-related set-ups (Figure 1) are suitable. The use of metal-coated tapered fibers or pipettes has been most popular^{3,4} and these have been used in commercial instruments⁵ and in numerous laboratory-made set-ups. However, it was not always appreciated that metal-coated tips produce enormous temperature gradients if they heat up to 100–500 °C,⁶ a fact that has recently been used to sublime off locally anthracene (**1**) vapor (melting point 218 °C; Cr-coated tip) from its crystal surface.⁷ Thus, the modes A, A', B' in Figure 1 can at best be used for heat-resistant surfaces lacking thermal effects, or possibly for measurements under water. Anyhow, the overwhelming part of the light that is coupled into the fiber is absorbed and transformed into heat by the metal coating and Al coatings may evaporate at the end of the tip.^{6b} However, metal-coated tapered tips have been used successfully for single molecule detection on flat surfaces when they were not used as the light source.⁸

A closer analysis of Figure 1 reveals that the evanescent approaches E, F and G [photon scanning tunneling microscopy (PSTM)] are unsuitable for rough and opaque samples. Only mode C, which uses uncoated tips that stay cold, is useful for rough opaque and transparent samples. Mode D requires transparency and the more recent approach with Lecher waveguide tetraeder probes⁹ requires flat samples. The reflection-back-to-the-fiber set-up (mode C) is highly versatile and so sensitive that not only inorganic and

* Correspondence to: G. Kaupp.

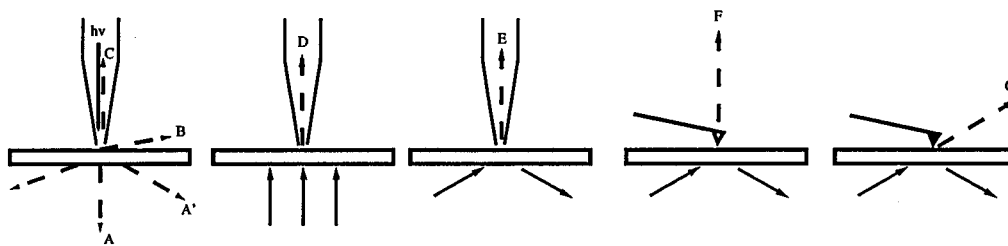


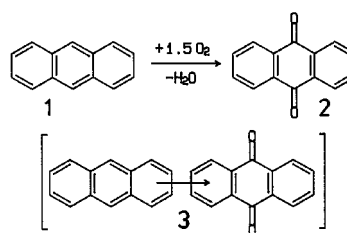
Figure 1. Basic geometries for SNOM (A, B, C, D) and PSTM (A', E, F, G). Illuminating light, solid arrows (sloping arrows from underneath, beyond the angle of total reflection); collected light, dashed arrows

polymer^{10–12} but also organic and possibly biological materials can be successfully probed. The images of this work have been taken with a commercial instrument that provides high feedback dynamics, allowing for fast scans of 50–125 $\mu\text{m s}^{-1}$ in the 10 μm range.¹³ Uncoated fiber tips are used, as is shown schematically in Figure 2. The polarizer increases the signal-to-noise ratio. The fiber tip with a nominal radius of ≤ 15 nm is dithered laterally and provides the 'shear-force' feedback signal. The large diameter of the illuminated spot, which may reach ≥ 1 μm ,¹⁴ does not impede high resolution, because the reflected light enters the tip in the near-field.¹⁰ Hence, only a small portion of the illuminated area contributes to the reflection signal and collection of reflected light works also at slopes that may reach 30° or more. SNOM measurements with uncoated tips yield reproducible and interpretable images which reveal variations of the chemical composition of non-uniform solid surfaces.

Organic crystals that were chemically modified by either partial autoxidation with oxygen or partial diazotization with nitrogen dioxide were chosen. Numerous such gas–solid reactions can be run quantitatively to 100% completion without waste formation.^{14–17} Hence, the elucidation of their mechanisms is of great importance because environmentally benign syntheses are badly needed for chemical production techniques of the future.

CHEMICAL CONTRAST IN AUTOXIDATIONS

The autoxidation products of anthracene (**1**) are anthraquinone (**2**) and water that evaporates from the surface. An intermediate oxidation state is the brown 1:1 charge-transfer complex **3** from the melt of **1** and **2**. It is only stable in the solid state and, unlike **1** and **2**, it absorbs strongly at 488 nm.



No SNOM contrast was obtained when probing (001) surfaces of **1** after exposure to air in a closed bottle for 6 months. No variations in reflectivity were found at 14 nm steps or at further (minor) defects. Hence, the surface was chemically uniform and had not autoxidized. The same was true for flat parts of pretreated (110) surfaces of **1** that did not show any significant variations of local reflectivity. The chemical non-reactivity on (001) and (110) derives from the inaccessibility of the reaction centers of **1** to oxygen, as imposed by the crystal packing. Thus, on (001) all molecules **1** stand steeply (67°) on their short edge, hiding both reaction centers, whereas on (110) half of the molecules stand steeply (76°) on their long edge, presenting only one of their central carbon atoms and shielding the rest of the molecules that stand on their long edges at a tilt of 23°. Both reaction centers of **1** are accessible only at faces that are skew to the natural ones.

Interestingly, the molecular packing on {110} seems to enhance the occurrence of crystal faults on that form, such as the 400 nm deep crater which is shown in the AFM topography in Plate 1(A). At the slopes, which rarely exceed 20° (some reach up to 30°), it is expected that both reaction centers of **1** are accessible to oxygen and that the analytically observed autoxidation occurs. It is perfectly clear that non-contact AFM alone is not able to show if the minor microcrystalline features in Plate 1(A) are chemically changed or not, their overall appearance being smooth and

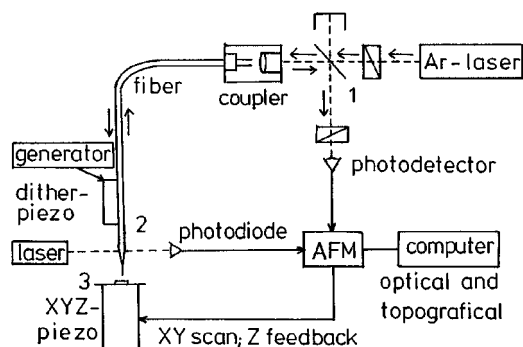
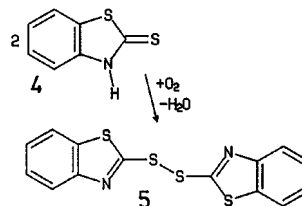


Figure 2. Block diagram of a reflection-back-to-the-fiber SNOM with shear-force distance control and cross-polarization detection system. (1) Beam splitter and crossed polarizers; (2) shear-force control system; (3) sample mounted on the piezo stage

inconspicuous. However, the SNOM image [Plate 1(B)] shows marked local variations of reflectivities which do not depict topography, but show chemical contrast due to three efficiencies of reflectivity, that is, 'normal' reflection from the flat part, increased reflection from the crystallites in the depths (also at the right corner) and at the left slope, and decreased reflection from some shallow slopes. The local variation of the reflectivity is clearly seen in the cross-sections. It is evident that we detect the response of the three different chemical species **1**, **2** and **3**. Chemical analyses exclude further products and the presumed labile primary 9,10-bridged peroxide of **1** has never been detected. The relative reflectivity properties are easily assigned to **1** (low,

unpolar), **2** (higher, polar) and **3** (very low, light absorbing at 488 nm).



Chemical contrast is also found in the solid-state autoxidation of 2-mercaptobenzothiazole (thioamide form **4**)¹⁹ on its (001) face. Chemical analyses indicate that bis-

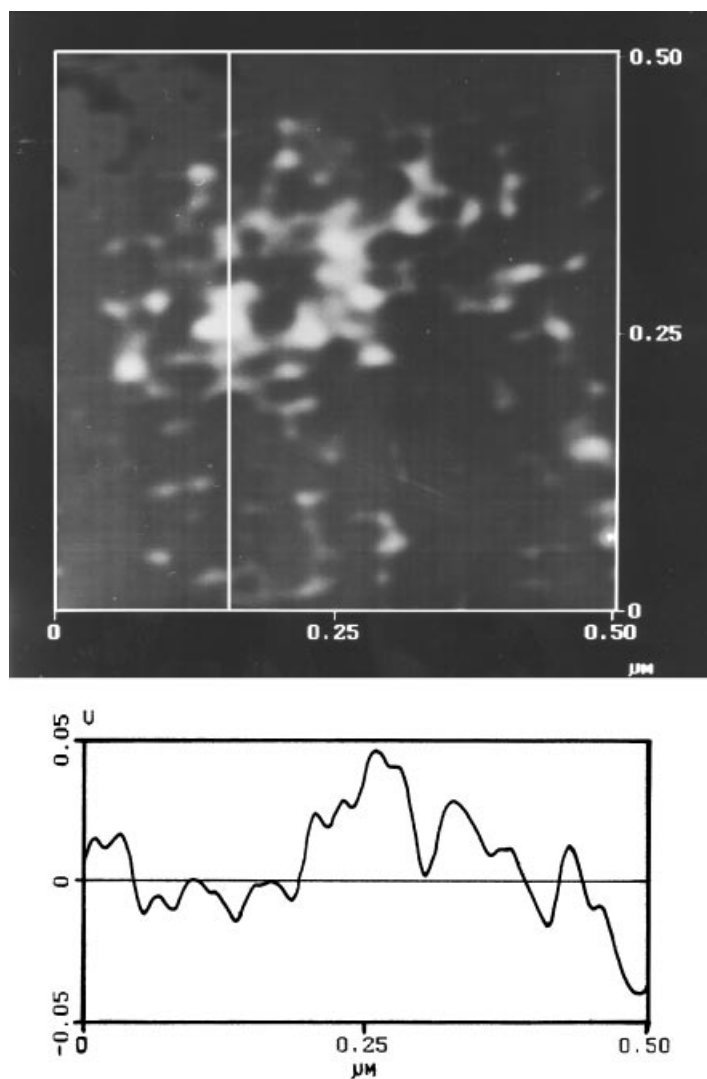


Figure 3. High-resolution reflection SNOM image (488 nm, arbitrary units of intensity) at a sloping (10–15°) autoxidation site on the (110) surface of **1**, showing peak-to-peak distances down to 18 nm

2-benzothiazolyl disulfide (**5**) and evaporating water are the only products. The crystal packing of **4** indicates that all relevant functional groups are efficiently shielded¹⁹ and thus not directly available on the surface layer. Therefore, such crystals protect themselves against autoxidation and are very stable in air. Islands are formed upon prolonged standing that consist of **5**. Apparently the autoxidation starts only at dislocations where the functional groups are accessible and then continues there. The central hill on the large island in Plate 2(A) is 350 nm high and the slopes at the shores are typically 20°. The SNOM image [Plate 2(B)] shows that the oxidation product **5** is less reflective than **4** in the near-field. Hence, the contours of the islands are precisely traced. However, there is no correlation with the island topography and it appears that the surface is chemically uniform on it. Outside the islands a different chemical uniformity obtains, and this is supported by the sharpness of the borderlines. The reflectivity differences between **4** and **5** are very minor. The chemical contrast is by no means a topographical one.

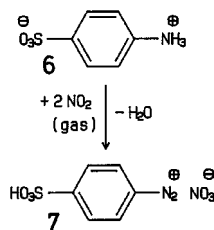
SNOM IN DIAZOTIZATION

The solid-state diazotization of sulfanilic acid monohydrate (**6**) has been studied by AFM¹⁵ and x-ray grazing incidence diffraction (GID)^{16a} on its most prominent (010) face. According to the crystal packing, that surface is not suitable for a complete diazotization reaction of **6** to give **7**. AFM and more directly depth-resolved in-plane GID show that the phase rebuilding proceeds sideways into the bulk from dislocations. This conclusion is supported by reflection SNOM at terrace steps on (010) of **6** after NO₂ treatment. Plate 3(A) shows the AFM topography {the unreacted slope on the surface of **6** [similarly to Plate 3(A)] did, of course, not give a SNOM contrast in the constant distance mode, as the surface was chemically uniform; cf. similar findings in Refs 6b and 16b} and Plate 3(B) the chemical contrast in SNOM: the terrace step exhibits stronger reflectivity. It is concluded that the diazonium salt **7** is formed at the slopes where the (hydrogen-bonded) amino groups of the molecular strings, that stand nearly vertical on (010), are accessible to the reacting gas NO₂. The flat part of the surface is only partly diazotized because half of the molecules **6** have their amino groups up, whereas the other half have them down in the bulk, and all molecules **6** are kept from moving up beyond the (010) surface by hydrogen bonding to the bulk.¹⁵ Still, the SNOM contrast is sufficiently large to discriminate clearly the different local chemical composition. All observations are in excellent agreement with the earlier conclusions.

RESOLUTION IN REFLECTION SNOM

The high resolution using thermally pulled tapered tips (CO₂ laser; radius 15 nm) in Figure 3 is obtained at topographic slopes of 10–15°, a fact that underlines the versatility of the reflection-back-to-the-fiber SNOM when combined with high feedback dynamics. A partly autoxi-

dized (110) surface of **1** was traced at high resolution. Very fine details of reflectivity are seen in Figure 3. The cross-section indicates peak-to-peak distances of as small as 18 nm. Thus, a resolution of at least 18 nm was achieved in ambient reflection SNOM using standard tips at a rate of 4 $\mu\text{m s}^{-1}$.



DISCUSSION

The local chemical contrast that has been demonstrated for the first time on three very different organic systems provides deep insights into the mechanisms of solid-state chemical reactions: the chemical contrasts show directly that the reactivity or non-reactivity depends sensitively on the molecular arrangement in the upmost molecular layer of the crystals. This is evident on different faces of anthracene (**1**) which, depending on the molecular alignment, were found to be unreactive ({001}; {110}) or reactive (skew to {110}). The same is observed macroscopically: very thin scales (8–10 μm) of **1**, which exhibits (001) faces almost exclusively, are much more stable in air than compact prisms of **1** with their most prominent {110} forms and many large dislocations on them. The autoxidation of 2-mercaptobenzothiazole (**4**) on (001) is only possible around dislocations which serve as starting points, because the molecular packing indicates shielding of the relevant functional groups. The SNOM investigations provide evidence that only the observed islands contain the reaction product **5**. Terrace steps are major sites of diazotization of sulfanilic acid (**6**) on (010), the hydrogen bonded strings of molecules being attacked from their sides. This cannot be seen in AFM topography but can be, very distinctly, with SNOM. Thus, important new evidence is gained which complements AFM and GID results. As reflection SNOM with slim uncoated tips under shear-force control does not experience topographical effects, proof of chemical uniformity or non-uniformity is obtained even in the presence of common surface features^{4,6b,14–18} that may reach μm heights. Such detailed mechanistic information is important for the continuing development of environmentally benign solid-state syntheses without producing wastes.

OUTLOOK

It is remarkable that near-field reflectivity differences between unlike absorbing or non-absorbing organic molecules can be distinguished very sensitively on very rough surfaces. Variations in detection wavelength or diffraction of the reflected light for local fluorescence^{11,20} and Raman

spectroscopy²¹ will further increase the information obtained with organic and, of course, biological material. The reflectivity will be useful for the discrimination of different physical states (crystals, polymers,²² layers,²³ etc.) and for all sorts of more strongly reflecting inorganic materials (metals, semiconductors, salts, oxides, ceramics, catalysts, doped surfaces, etc.). Contrast of materials in composites or polymer blends will also be easily detectable. Hence, the present results offer promise for wide applications of reflection-back-to-the-fiber SNOM using slender and cold uncoated tips instead of blunt and hot metal-coated tips.

ACKNOWLEDGEMENTS

We thank Professor D. A. Smith, Leeds, for providing access to his SNOM equipment and Professor H. Fuchs, Münster, for making accessible his pipette puller. The Deutsche Forschungsgemeinschaft is thanked for a travel grant.

REFERENCES

1. E. A. Ash and G. Nicholls, *Nature (London)* **237**, 510 (1972); R. Young, J. Ward and F. Scire, *Rev. Sci. Instrum.* **43**, 999 (1972); W. D. Pohl, W. Denk and M. Lanz, *Appl. Phys. Lett.* **44**, 651 (1984); G. Massey, *Appl. Opt.* **23**, 658 (1984); U. C. Fischer, *J. Vac. Sci. Technol. B* **3**, 386 (1985).
2. G. Binnig, C. F. Quate and Ch. Gerber, *Phys. Rev. Lett.* **56**, 930 (1986).
3. E. Betzig, M. Isaacson and A. Lewis, *Appl. Phys. Lett.* **51**, 2088 (1987); S. I. Bozhevolnyi, O. Keller and M. Xiao, *Appl. Opt.* **32**, 4864 (1993); R. Toledo-Crow, P. C. Yang, Y. Chen and M. Vaez-iravani, *Appl. Phys. Lett.* **60**, 2957 (1992).
4. G. Kaupp, *Adv. Photochem.* **19**, 119 (1995).
5. These are AURORA[®] I/II of TopoMetrix, Santa Clara and NANONICS[®] of Nanonics, Jerusalem.
6. (a) A. H. LaRosa, B. I. Jakobson and H. D. Hallen, *Appl. Phys. Lett.* **67**, 2597 (1995); (b) G. Kaupp, A. Herrmann and M. Haak, *lecture at NFO-4, Jerusalem*, February 13, 1997, *Ultramicroscopy* 1997, in press.
7. D. Zeisel, S. Netterheim, B. Dutoit and R. Zenobi, *Appl. Phys. Lett.* **68**, 2491 (1996).
8. G. Tarrach, M. A. Bopp, D. Zeisel and A. J. Meixner, *Rev. Sci. Instrum.* **66**, 3569 (1995).
9. J. Koglin, U. C. Fischer and H. Fuchs, *J. Biomed. Opt.* **1**, 75 (1996); U. C. Fischer, J. Koglin, A. Naber, A. Raschewski, R. Tiemann and H. Fuchs, *NATO ASI Series*, No. **314**, p. 309. Kluwer, Dordrecht (1996).
10. M. Spajer, D. Courjon, K. Sarayedine, A. Jalocha and J.-M. Vigoureux, *J. Phys. (Paris) Ser. III* **1**, 1 (1991).
11. H. Bielefeldt, I. Hörsch, G. Krausch, M. Lux-Steiner, J. Mlynek and O. Marti, *Appl. Phys. A* **59**, 103 (1994).
12. G. Krausch, S. Wegscheider, A. Kirsch, H. Bielefeldt, J. C. Meiners and J. Mlynek, *Opt. Commun.* **119**, 283 (1995).
13. Instrument: RASTERSCOPE SNOM of DME, Copenhagen; G. Kaupp, A. Herrmann and M. Haak, *J. Vac. Sci.* in press.
14. G. Kaupp, J. Schmeyers, M. Haak, T. Marquardt and A. Herrmann, *Mol. Cryst. Liq. Cryst.* **276**, 315 (1996).
15. G. Kaupp, J. Schmeyers, M. Haak and A. Herrmann, *Labo-Trend* **95**, 57 (1995); English translation in WWW under <http://kaupp.chemie.uni-oldenburg.de>.
16. (a) A. Herrmann, G. Kaupp, T. Geue and U. Pietsch, *Mol. Cryst. Liq. Cryst.* **293**, 261 (1997); (b) G. Kaupp, in *Comprehensive Supramolecular Chemistry*, edited by J. E. D. Davies, Vol. 8, p. 381. Elsevier, Oxford (1996); *Chemie in unserer Zeit* **31**, 129 (1977); English translation in WWW under <http://kaupp.chemie.uni-oldenburg.de>.
17. G. Kaupp and J. Schmeyers, *J. Org. Chem.* **60**, 5494 (1995).
18. G. Kaupp and M. Plagmann, *J. Photochem. Photobiol.* **80**, 399 (1994).
19. J. P. Chesick and J. Donohue, *Acta Crystallogr. Sect. B* **27**, 1441 (1971).
20. D. A. McL. Smith, S. A. Williams, R. D. Miller and R. M. Hochstrasser, *J. Fluoresc.* **4**, 137 (1994); R. X. Bian, R. C. Dunn, X. S. Xie and P. T. Leung, *Phys. Rev. Lett.* **75**, 4772 (1995); E. Monson, G. Merritt, S. Smith, J. P. Langmore and R. Kopelman, *Ultramicroscopy* **57**, 257 (1995).
21. D. A. Smith, S. Webster, M. Ayad, S. D. Evans, D. Fogherly and D. Batchelder, *Ultramicroscopy* **61**, 247 (1995).
22. H. Ade, R. Toledo-Crow, M. Vaez-iravani and R. J. Sponak, *Langmuir* **12**, 231 (1996).
23. D. A. Higgins, P. J. Reid and P. F. Barbara, *J. Phys. Chem.* **100**, 1174 (1996).

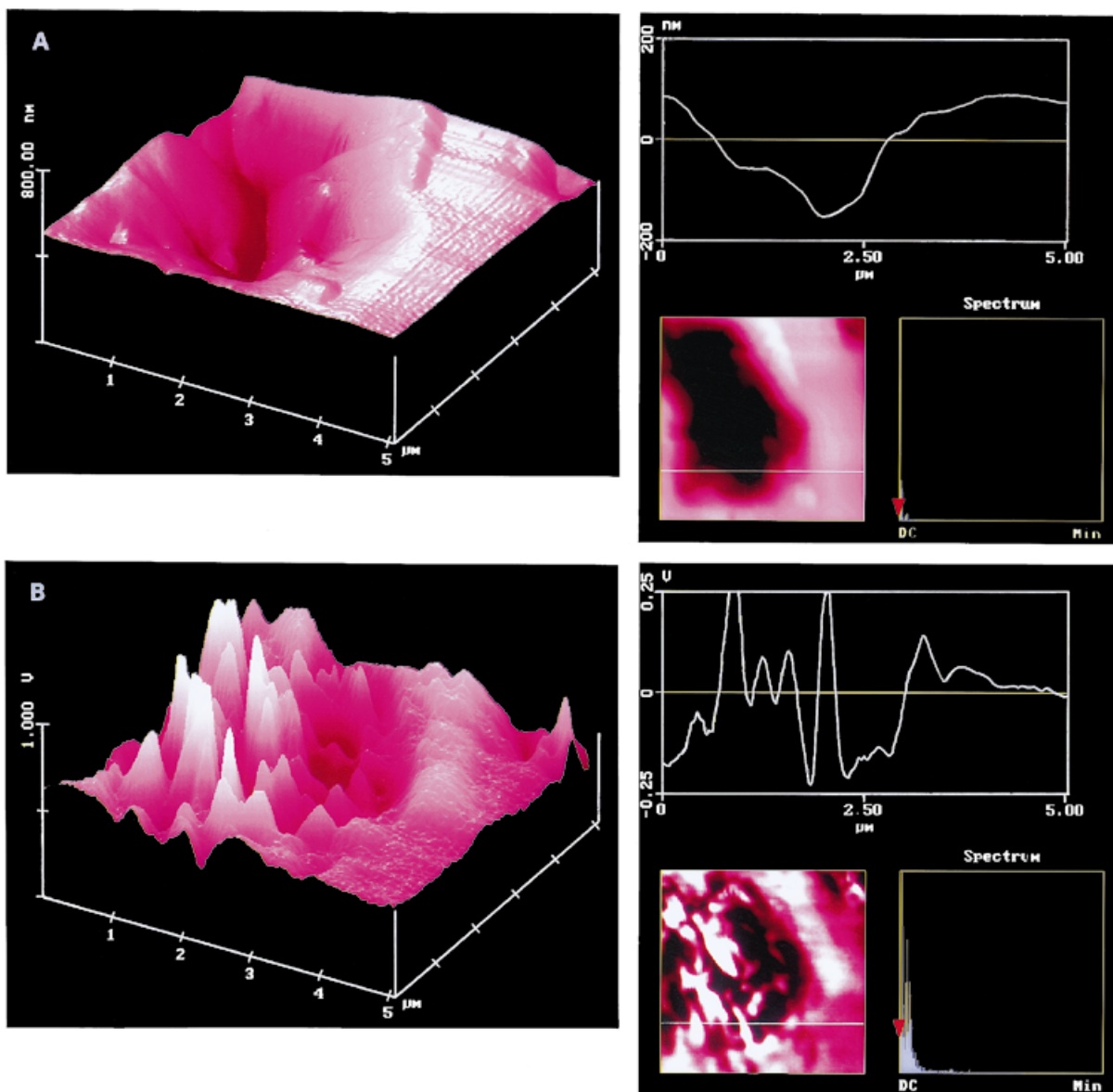


Plate 1. Simultaneous shear-force AFM topography calibrated with a 3000 (X,Y)/500 (Z) nm gold grating (A) and reflection SNOM image (arbitrary units) taken with 488 nm light (B) of a partially autoxidized (110) surface of anthracene (**1**) ($P2_1/a$) at a 400 nm deep crater site

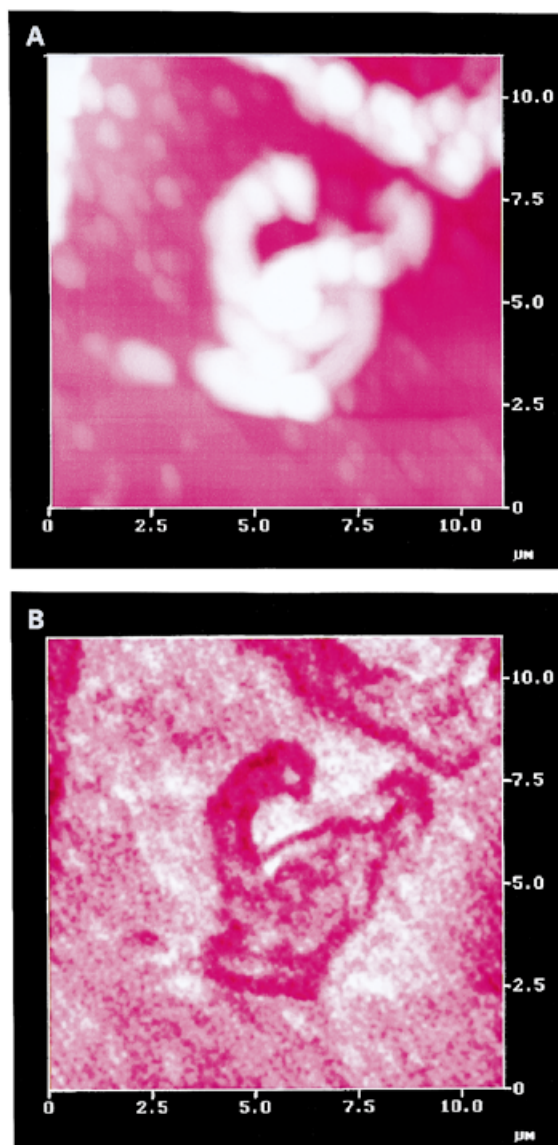


Plate 2. Simultaneous shear-force AFM topography (the contrast covers height differences of 500 nm) (A) and reflection SNOM image (arbitrary units of intensity) taken with 488 nm light (B) of **4** ($P2_1/c$) on (001), showing islands generated by autoxidation to give the less reflecting disulfide **5** solely on the islands

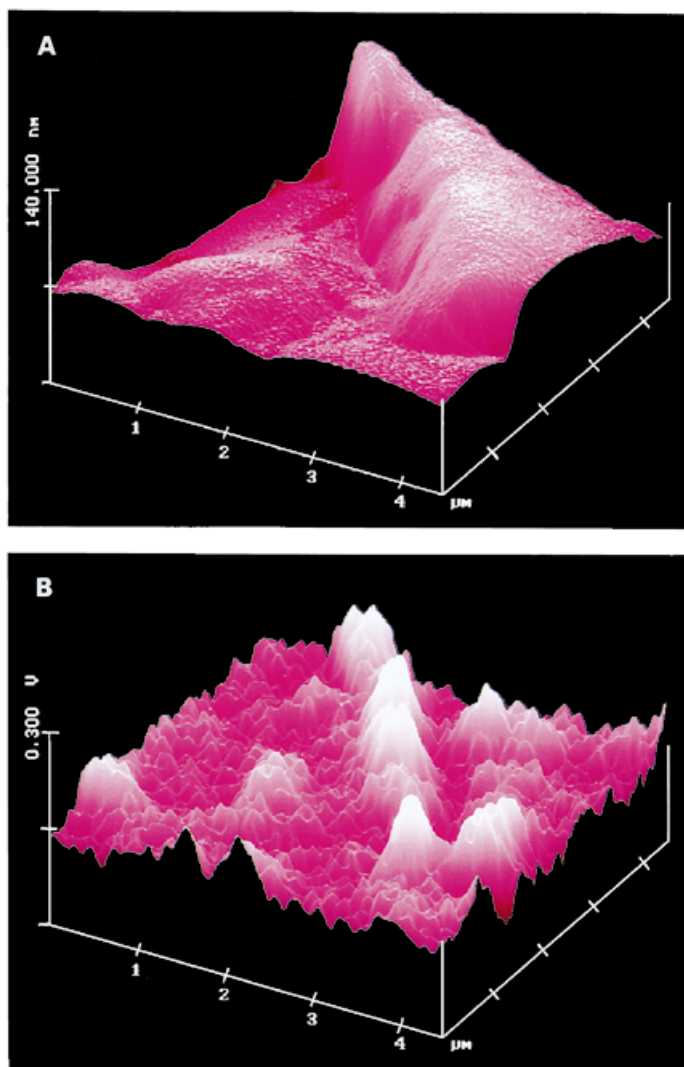


Plate 3. Simultaneous shear-force AFM topography (A) and reflection SNOM image taken with 488 nm light (B) of sulfanilic acid monohydrate (**6**) (*P*₂₁/*c*) on the (010) face, that had a terrace step of 50-90 nm height on it, after 1 min of treatment with 1 cm³ of NO₂ (1:4 mixture with air injected from a 1 cm distance), yielding the diazonium salt **7** which is formed at the slopes and reflects more strongly